FRACTURE TOUGHNESS AND MICROSTRUCTURE OF S.A.W. WELD METAL

L. DEVILLERS - B. MARANDET - D. KAPLAN - A. RIBES - P.V. RIBOUD

Institut de Recherches de la Sidérurgie Française (IRSID)

The fracture toughness of C-Mn weld metal (S.A.W) has been assessed from the transition regime up to the upper shelf with the help of Charpy impact tests and the J-integral concept. The weld metal oxygen content has a strong influence on the resistance to brittle fracture and the resistance to ductile crack extension. The results are interpreted in terms of weld metal oxide inclusions and weld metal microstructure.

INTRODUCTION

Weld metal is usually considered as a preferential site for the initiation and propagation of brittle fracture in H.S.L.A. steel structures (1, 2). Weld metal toughness requirements are specially hard to meet in the case of high heat input single pass processes such as submerged arc welding (S.A.W.). This process is characterized by high dilution of the base metal (60 to 70 %) and low cooling rates which have a tendency to promote low toughness microstructure s in the weld metal (3, 4). Nevertheless it has been clearly established that proper selection of the welding flux can improve drastically the toughness of the weld metal(5, 6, 7, 8). Welding fluxes are made of various oxides and must be used to ensure the stability of the arc. Furthermore they act as a slag covering the liquid metal and may have strong metallurgical effects on the weld metal properties (9, 10, 11, 12). Large amounts of oxygen, from 20 to 100 x 10^{-3} % according to the flux composition, are picked up by the weld metal from the flux. These large oxygen contents have been shown to have an effect on the weld metal microstructure (13 - 18), yielding in some cases a fine "acicular ferrite" structure which displays a good toughness at low temperatures.

We present here the results of a study on the S.A.W. weld metal toughness as a function of its oxygen content. The results are interpreted in terms of weld metal inclusions and microstructures.

EXPERIMENTAL METHOD

Unless otherwise stated, the results have been obtained with one 20 mm thick H.S.L.A. plate and one welding wire whose compositions are indicated in table 1 along with the welding parameters, base plate properties and some examples of welding fluxes and weld metal compositions. The welding conditions and welding products are relevant to industrial practice. The various weld metals have undergone identical welding thermal cycles and differ mainly in their oxygen contents depending on the welding fluxes used. It has be noted that no post weld heat treatment has been applied and that the fluxes used allowed no significant transfer of microalloying elements such as titanium and boron.

Charpy impact tests and J_{Ic} measurements were carried out at different temperatures to assess the fracture toughness of weld metal from the brittle (cleavage) up to the fully ductile regime. J_{Ic} measurements were performed on fatigue precracked single edge notched specimens (S.E.N. B x 2B) 170 x 35 x 17,5 mm, in size. The tests have been conducted in a large temperature range (from -120°C up to +60°C) and the load-displacement curves were interpreted according to the A.S.T.M. E 813-81 standard. J integral was calculated at initiation of stable or unstable crack extension from the following (19) :

$$J = \frac{2\,U}{B(W-a_o)} \quad (J \text{ in } MJ/m^2)$$

where U = area under load - load point displacement record in energy units

B = specimen thickness

W = specimen width

a_o = original crack length, including fatigue precrack

The A.C. potential drop method (20) was used to detect initiation of ductile crack extension during loading. In this paper :

- $J_{Ic\,f}$ stands for J_{Ic} measured at initiation of unstable crack extension by cleavage,
- $J_{Ic\,i}$ stands for J_{Ic} measured at initiation of stable crack extension by ductile tearing.

The corresponding stress intensity factor K_{Jc} is calculated from :

$$K_{Jc} = \sqrt{\frac{E}{1-\nu^2}\,J_{Ic}} \quad (K_{Jc} \text{ in } MPa\sqrt{m})$$

where E = Young's modulus

ν = Poisson's ratio

We have determined the $J_R - \Delta a$ crack resistance curve in the fully ductile regime (+60°C) by the interrupted loading method, as described in the ASTM E 813-81 standard. According to this standard, the critical J_{Ic} value at initiation of ductile crack extension ($J_{Ic\,i}$) is obtained conventionally at the intersection of the best fit line (adjusted on the $J_R - \Delta a$ values included between two offset-lines) and the theoretical blunting line $J = 2\,\sigma_{flow}\,\Delta a$.

J_{Ic} values determined by this method are compared to J_{Ic} values obtained at initiation by the A.C. potential drop method.

RESULTS

As stated above, the weld metal oxygen content is strongly dependent on the chemical composition of the welding flux. The flux is either fused or agglomerated and consists mainly of oxides (table 1). We have assumed that the amount of less stable oxides in the flux would control the quantity of oxygen picked up by the weld metal from the liquid slag layer during welding. Among such oxides (21) SiO_2 and MnO may be found in large amounts in commercial fluxes. Figure 1 shows a clear relationship between the weld metal oxygen content measured in our experiments and the total percentage of SiO_2 and MnO in the flux. Hence the oxygen level of the weld metal can be estimated from the flux composition.

Weld metal oxygen will combine with deoxidants brought into the weld metal through base plate dilution and will form inclusions. These inclusions have a detrimental effect on the resistance to ductile fracture. Figure 2 a shows that the Charpy upper shelf energy decreases when the weld metal oxygen content (i.e. inclusions content) increases.

A more appropriate description of the resistance to ductile crack extension in relation with the oxygen content is given in figure 2b by the $J_R - \Delta a$ curves. These results were obtained at 60°C for two oxygen levels (40 and 80 x 10^{-3} %). As expected from the Charpy V notch tests in the upper-shelf, it appears clearly that increasing the oxygen level reduces markedly the tearing modulus $T = \frac{dJ}{da} \frac{E}{\sigma_{flow}^2}$ in the crack propagation regime. Furthermore, J_{Ic} values derived from the ASTM E 813-81 method are significantly different while the A.C. potential drop method yields similar J_{Ic} values at initiation for the two materials. In fact, direct S.E.M. observations of fracture surfaces indicate clearly that physical initiation of ductile crack extension takes place at J values lower than that derived from the $J_R - \Delta a$ resistance curve, according to the A.S.T.M. recommendation.

To design safe welded structures, the brittle fracture of weld metal is of greater concern than ductile fracture. We have shown that the resistance to brittle fracture does not decrease continuously with oxygen content but reaches a maximum at a critical oxygen level. This appears in figure 3a vhere Charpy transition temperatures are plotted against the oxygen content. The weld metal transition temperatures can be much lower than those of Heat Affected Zones (H.A.Z.) submitted to the same thermal cycles and having similar compositions but for their lower oxygen content ($\sim$ 5 x 10^{-3} %) (figure 3a).

The K_{Jc} fracture toughness tests conducted at different temperatures on fatigue precracked specimens cônfirm the influence of oxygen content as observed with Charpy specimens (figure 3b). The fracture toughness transition temperatures for the two oxygen levels considered (40 and 80 x 10^{-3} %) are in satisfactory agreement with the Charpy transition temperatures as infered from the correlation established previously for base metals (22). It appears therefore that the fracture toughness $K_{Jc\,f}$ is strongly influenced in the transition regime (cleavage) by the oxygen content. The influence of the oxygen content on fracture toughness ($K_{Jc\,i}$) at initiation of ductile tearing is much reduced in the upper shelf regime, as indicated above. The results of figure 3a have been checked by welding other H.S.L.A. plates of similar composition. It appears that the critical oxygen level depends on the amount of deoxidants brought into weld metal through base plate dilution. Figure 4 shows that, according to our results, the critical oxygen content which yields the highest resistance to brittle fracture, increases with the base plate aluminium content.

DISCUSSION

Weld metal oxygen combines with deoxidants to form inclusions. To predict the nature and amount of these inclusions we have resorted to a thermodynamics model whose results are supported by direct T.E.M. examinations and X ray microanalysis of weld metal (23). The model describes the weld metal behaviour as it cools down to 1500°C. It takes into account data of the Fe-Al-Si-Mn-O phase diagram, assuming that the equilibrium is reached at successive decreasing temperatures during cooling. Table 2 indicates the results obtained in our experimental conditions i.e. fixed base plate and wire compositions but various amounts of weld metal oxygen. For each oxygen level, we have obtained the amount and nature of inclusions formed : aluminium oxide up to 40 x 10^{-3} % oxygen and silicon - manganese - aluminium compound oxides above. It can be observed that this change in inclusions nature occurs around the oxygen level yielding the highest weld metal resistance to brittle fracture. Equivalent results have been obtained for other base plate aluminium contents.

The nature of weld metal inclusions has been observed directly by T.E.M. of carbon replica with X ray microanalysis of extracted inclusions. Some examples are shown in figure 5. Inclusions sizes range from 0.1 to 2 microns in all specimens examined. At lower oxygen levels, most inclusions are aluminium oxides ; they are sharp cornered since they occur as solid precipitates within the liquid metal. Above 40×10^{-3} % oxygen, all inclusions are compound oxides of aluminium, silicon and manganese ; they are globular since they occur as liquid precipitates within the liquid metal. Their precise compositions depend on the amount of oxygen in the weld metal. These observations substantiate the results of our thermodynamics model.

The resistance to ductile crack growth is known to decrease when the number of inclusions per unit volume increases (24, 25). So far we have not assessed the precise inclusions sizes distribution in our experiments. Nevertheless, it seems that it does not vary much from one specimen to another according to their oxygen contents. Increasing the oxygen content would therefore mean increasing the volume fraction of inclusions and this would account for the effect shown in figure 2. S.E.M. examinations revealed no drastic change in the ductile fracture surface appearance according to the inclusions content. As shown in figure 6, it is possible to observe isolated globular inclusions at the centres of the fracture surface dimples.

As stated before, the resistance of weld metal to brittle fracture has been related to its microstructure. The tougher weld metal microstructure contains a high percentage of fine interlocking ferrite grains usually referred to as "acicular ferrite" by welding metallurgists. Coarsening of this structure and the presence of large proeutectoïd ferrite veins at prior austenite grain boundaries drastically deteriorate the weld metal toughness (3, 15). This is confirmed by our results ; some examples of microstructures corresponding to different oxygen levels are shown in figure 7.

The question now arises to know how the nature of oxide inclusions may be related to the weld metal microstructure, in order to account for the results described above. We have first assessed the effect of oxide inclusions on the austenite grain size. We have reheated weld metal specimens up to 1300°C and 1400°C on a "Gleeble" R.P.I. machine. Specimens were heated up to the peak temperature in 3 seconds, hold for 15 seconds and then water quenched. At 1300°C the weld metal austenite grain size is of the order of 50 microns whatever the oxygen content within the range 20 to 100×10^{-3} %. Base metal of similar composition but low oxygen level displays a 150 microns austenite grain size when submitted to the same treatment. The austenite grain growth seems to be impeded by oxide inclusions up to 1300°C in all the weld metal specimens. At 1400°C the weld metal austenite grain size depends on its oxygen content : 100 to 150 microns up to 50×10^{-3} % oxygen against 50 microns at higher oxygen levels (figure 8). High oxide inclusions contents may be able to induce finer austenite grain size. This in turn would slightly raise up the transformation temperature and furthermore would markedly increase the density of grain-boundary nucleated ferrite. As stated above the proeutectoïd ferrite veins are known to reduce the resistance to brittle fracture.

Further experiments have allowed us to observe the ferrite nucleation during the austenite transformation. Weld metal specimens have been submitted to heat treatments up to 1400°C to simulate welding. The controlled cooling (Δt_{300}^{700} = 120 s) has been interrupted by quenching to room temperature from 575°C. This procedure makes it possible to observe the nucleation sites for ferrite at different oxygen levels as shown in figure 9. Below the critical oxygen level, ferrite nucleation occurs mainly at austenite grain boundaries resulting in large elongated ferrite grains. Around the critical oxygen level, ferrite nucleation occurs both at austenite grain boundaries and at numerous sites within the grains. As suggested by other authors (15, 26), these nucleation sites may be oxide inclusions as indicated in figure 10. This enhanced nucleation results in fine interlocking ferrite particles impeding each other's growth. At higher oxygen levels, intragranular nucleation of ferrite becomes more sluggish and the finer austenite grain size increases the amount of grain boundary nucleated ferrite.

To assess more precisely the nature of weld metal microstructure at different oxygen levels we have prepared thin foils for T.E.M. The weld metals had oxygen contents of 27, 48 and 82×10^{-3} % i.e. below, around and above the critical oxygen level. In all the specimens, the microstructures are composed essentially of elongated ferrite grains indispersed with carbide-ferrite agregates or in some cases retained austenite. The structures of 27 and 82×10^{-3} % oxygen weld metals are practically identical and we present for comparison in figure 11 some micrographs of the 48 and 82.10^{-3} % oxygen weld metals. The ferrite grains are significantly finer in the tougher weld metal (48×10^{-3} % oxygen), suggesting that intragranular ferrite nucleation was indeed enhanced in this case. In the sample containing 82.10^{-3} % oxygen, electron diffraction showed some constituents that could be retained austenite or a compound M.A. (martensite-austenite). Figure 12 suggests that at this 48.10^{-3} % oxygen level, intragranular ferrite nucleation may have occurred at oxide inclusions. At the higher and lower oxygen levels, the ferrite grains do not seem to be related to the oxide inclusions. The lathlike ferrite grains observed are probably the result of grain boundary nucleation.

CONCLUSION

According to the amount of oxygen provided by the flux and the amount of deoxidants provided by the parent steel plate, S.A.W. weld metal contains various amounts of different oxide inclusions which have been identified. These inclusions have significant effects on weld metal toughness.

In the ductile regime, increasing the amount of oxide inclusions reduces the resistance to ductile crack extension without altering the J_{IC} values at initiation.

Furthermore the oxide inclusions have some influence on the weld metal microstructure. The higher oxide inclusions contents restrain the austenite grain growth at very high temperatures. This increases the density of proeutectoïd ferrite veins which are detrimental to the weld toughness in the transition regime. Additionally it raises slightly the transformation temperatures yielding coarser ferrite structures.

On the other hand, some particular oxide inclusions appear to favor the intragranular nucleation of ferrite, thus yielding a much finer and tougher microstructure.

As expected from these two opposite effects a "critical oxygen level" provides the higher weld metal toughness in the transition regime.

Acknowledgements

The authors are indebted to Dr. B. THOMAS for a critical discussion of this investigation.

Sincere thanks are here expressed to Mr. C. ROUX, D. BOULEAU and B. LALOI who have carried out the experimental part of the project.

This work was part of and E.C.S.C. project.

REFERENCES

1. De Roo, P. et al., 4th S.F.M.-S.I.S. meeting, Marseille, mai 1981. Publication de la soudure autogène française 32 bld de la Chapelle, Paris.
2. Masubuchi, K., "Analysis of welded structures", Pergamon Press, volume 33, 1980.
3. Bernard, G., Faure, F., Final report E.C.S.C. project 6710-93/3/304 EUR 5866.
4. Dorschu, K., Stout, R.D., Welding Journal, March 1961, p. 97 s.
5. Devillers, L., Riboud, P.V., I.I.W. document IX-1218-81.
6. Mori, N. et al., I.I.W. document IX-1196-81.
7. Palm, J.H. Welding Journal, July 1972.
8. North, T.H. et al. "Pipeline and Energy plant piping conference" W.I. of Canada, Calgary, November 1980.
9. Tuliani, S.S. et al., Welding and metal fabrication, July 1972.
10. Tuliani, S.S. et al., Welding and metal fabrication, August 1969.
11. Eagar, T.W., Welding Journal, March 1978.
12. Widgery, D.J., W.I. conference "Trends in steels and consumables for welding", London, November 13-16, 1978.
13. Tenkula, J., Ikkinen, V.K.H., Welding Research International, volume 8, 1978, n° 5.
14. Craig, J. et al. W.I. conference "Trends in steels and consumables for welding", London, November 13-16 1978.
15. Abson, D.J., Dolby, R.E. et al., Ibidem.
16. Cochrane, R.C., Kirkwood, P.R., Ibidem.
17. Ito, Y. et al., Sumitomo search n° 16, November 1976.
18. Ito, Y. et al., I.I.W. document IX-1194-81.
19. Rice, J.R. et al., A.S.T.M.-S.T.P. 536, 1973, p. 231-245.
20. Marandet, B., Sanz, G., A.S.T.M.-S.T.P. 631, 1977, p. 462-476.
21. Richardson, F.D., Jeffes, T.H.E., J.I.S.I., 160, 261, 1948.
22. Marandet, B., Sanz, G., A.S.T.M.-S.T.P. 631, 1977, p. 72-95.
23. Riboud, P.V. et al., Revue de Métallurgie-C.I.T., novembre 1981.
24. Edelson, B.I., Baldwin, W.M., Journal Transaction A.S.M. Quarterly, 55, n° 1, 1962, 230.
25. Roesch, L. et al., Mémoires Scientifiques de la Revue de Métallurgie, novembre 1966, 63, n° 11, p. 927-940.
26. Barritte, G.S. et al., "Quantitative microanalysis with high spatial resolution", Metals Society Book 277, 1981.

TABLE 1

1.a : Welding conditions :

	D.C. Wire	A.C. Wire
U	32 volts	36 volts
I	900 amps	930 amps
v	1 m/mn	1 m/mn
Δt_{300}^{700}	120 seconds	

1.b. : Compositions of base plate, wire, weld metals (10^{-3} W %)

	C	Mn	Si	S	P	Al	Mo	N	O	Nb
Base plate *	173	1415	268	12	13	53	-	9	2	37
Wire	70	1000	20	20	10	-	500			-
Examples of weld metal	145	1160	280	10	14	31	265	7	27	24
	151	1280	320	13	16	30	160	7	44	34
	133	1330	370	12	17	26	165	8	67	18

* base plate : YS = 395 MPa, UTS = 560 MPa, TK_{28J} = -65°C

1.c. : Examples of fluxes compositions (W %)

SiO_2	P_2O_5	Al_2O_3	CaO	Na_2O	K_2O	MnO	MgO	TiO_2	FeO	CaF_2
39	0.1	2.5	21	-	-	20	3	3	1	10
26	0.1	22	10	1	1	8	16	3	1	12
15	0.1	17	8	0.1	2	0.3	30	1	2	21

TABLE 2 - Predictions of the nature and amounts of oxides inclusions in our experimental conditions as a function of oxygen content.

Total oxygen content (10^{-3} W %)	Dissolved oxygen at equilibrium at 1500°C (10^{-3} W %)	Dissolved aluminium at equilibrium at 1500°C (10^{-3} W %)	Inclusions types at equilibrium at 1500°C	Amount of inclusions (10^{-3} W %)
10	0.18	26	aluminium oxide	21
20	0.26	14.8	"	42
30	0.60	0.40	"	62
40	2.7	0.41	aluminium oxide + compound oxides of Al, Si, Mn	78
50	2.9	0.37	"	96
60	4.2	0.17	compounds oxides of Al, Si, Mn	113
70	4.2	0.16	"	132

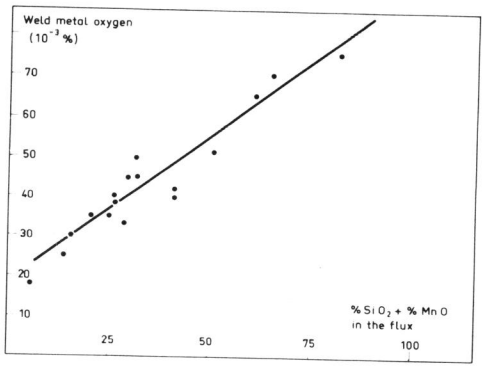

Fig. 1 : Variation of weld metal oxygen with % SiO_2 + % MnO in the flux.

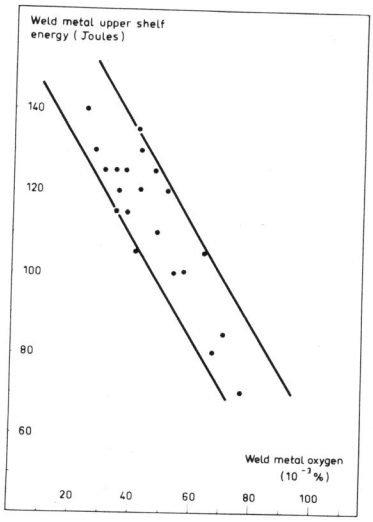

Fig. 2a : Charpy V upper shelf energy versus oxygen content.

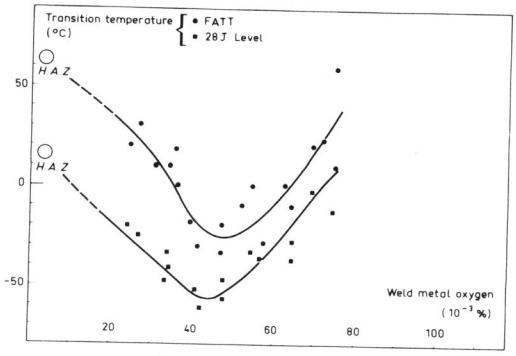

Fig. 3a : Charpy V transition temperatures as a function of oxygen content.

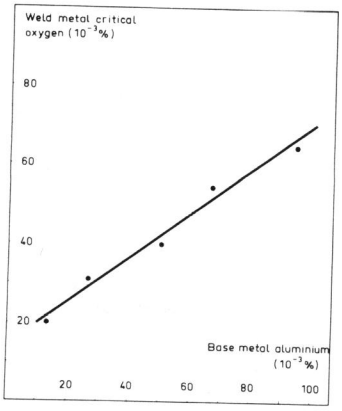

Fig. 4 : Weld metal critical oxygen content versus base metal aluminium content.

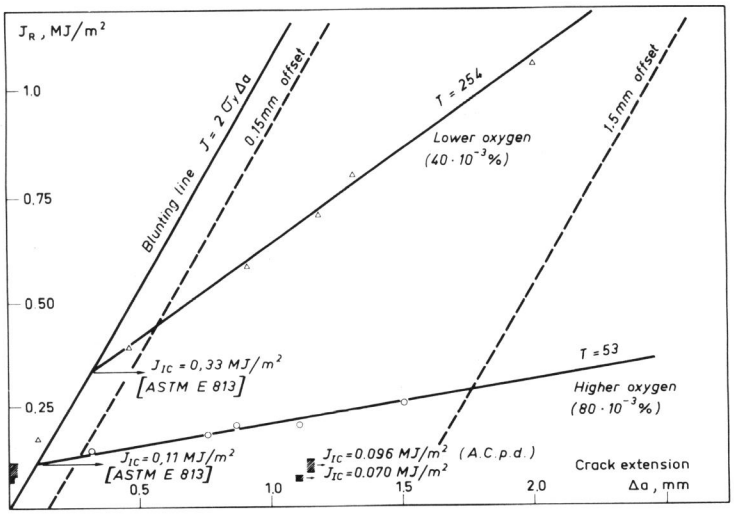

Fig. 2b – J_R – Δa curves for two oxygen levels (+60°C).

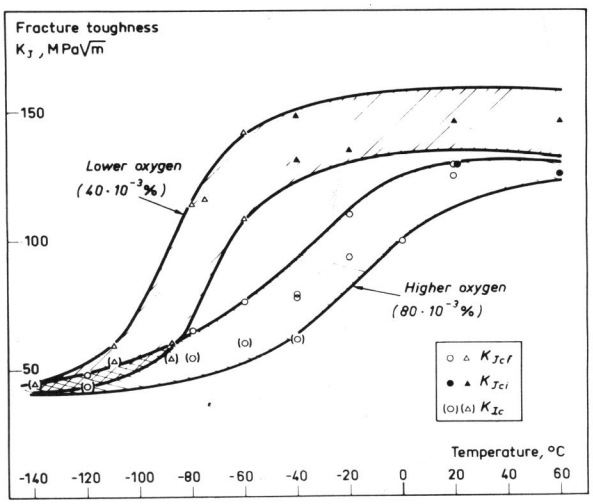

Fig. 3b : Fracture toughness as a function of temperature for two oxygen levels.

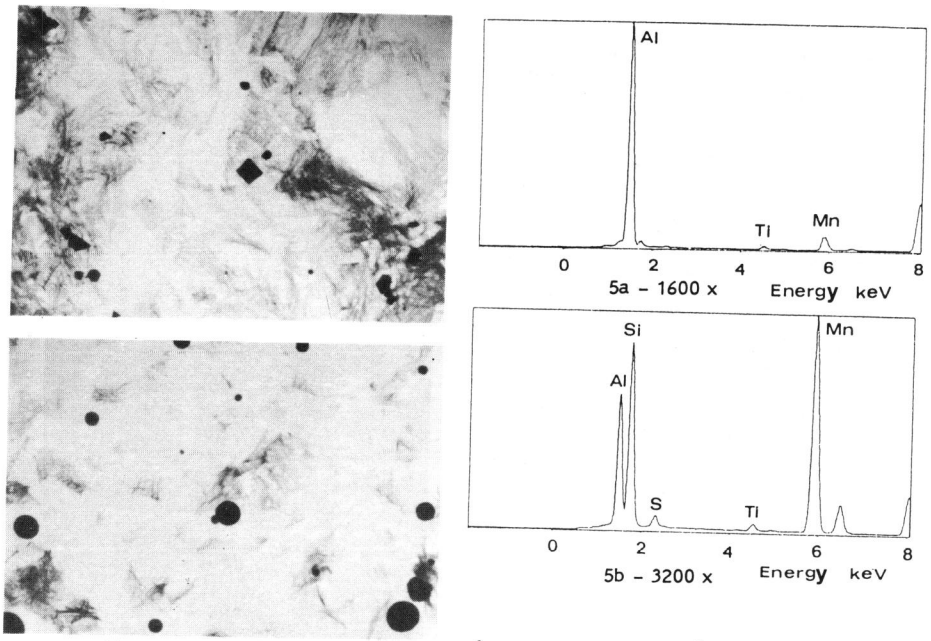

Fig. 5 : Oxide inclusions a) 27×10^{-3} % O_2, b) 67×10^{-3} % O_2.

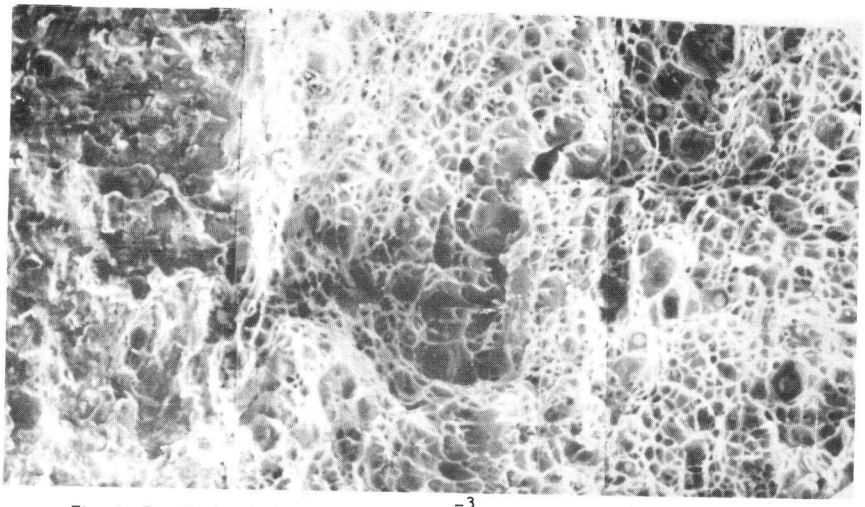

Fig. 6 : Ductile fracture surface - 80×10^{-3} % O_2 - S.E.M. - 800 x.

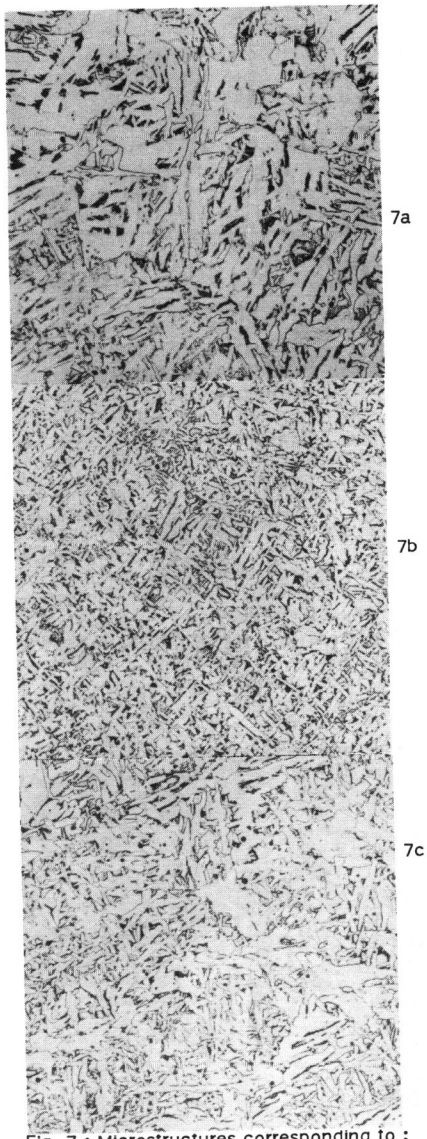

Fig. 7 : Microstructures corresponding to :

a) 27×10^{-3} % O_2

b) 44×10^{-3} % O_2

c) 67×10^{-3} % O_2

500 x

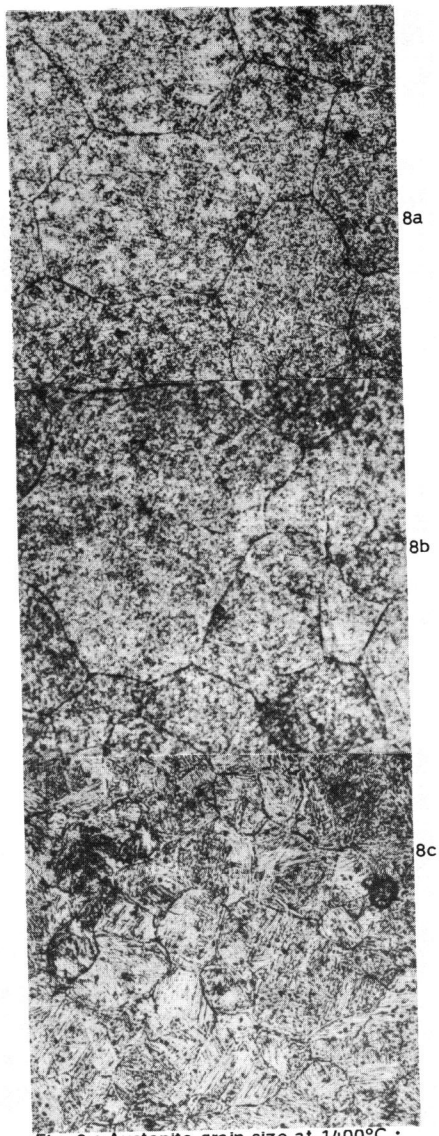

Fig. 8 : Austenite grain size at 1400°C :

a) 28×10^{-3} % O_2

b) 44×10^{-3} % O_2

c) 68×10^{-3} % O_2

200 x

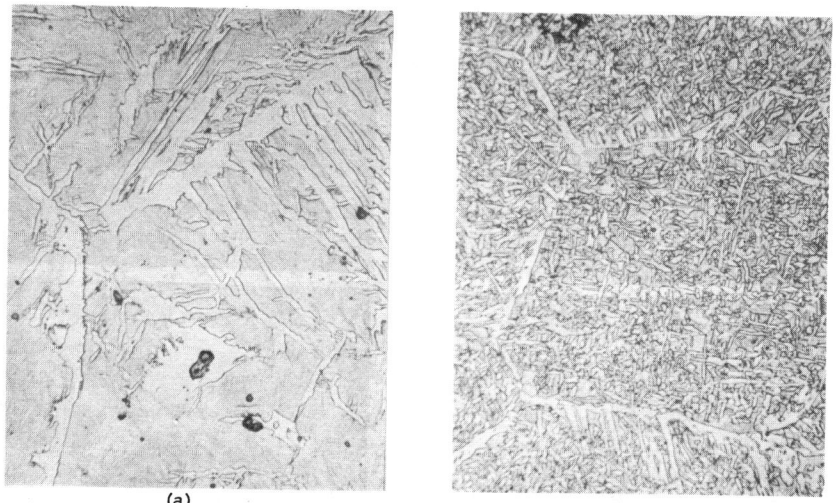

(a) (b)

Fig. 9 : Nucleation of ferrite
a) 27×10^{-3} % O_2
b) 44×10^{-3} % O_2 500 x

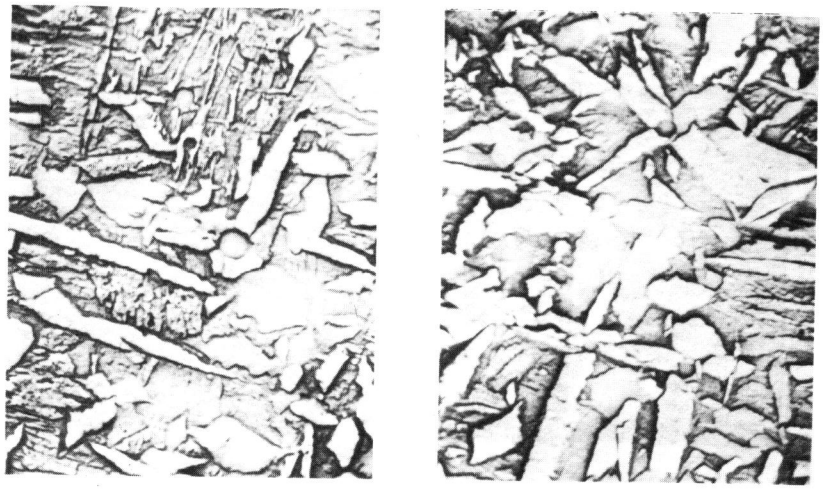

Fig. 10 : Possible nucleation of ferrite at oxide inclusions - 44×10^{-3} % O_2 - S.E.M. - 5000 x.

a b

Fig. 11 = Microstructures (T.E.M.) :
a) 48×10^{-3} % O_2
b) 80×10^{-3} % O_2 3600 ×

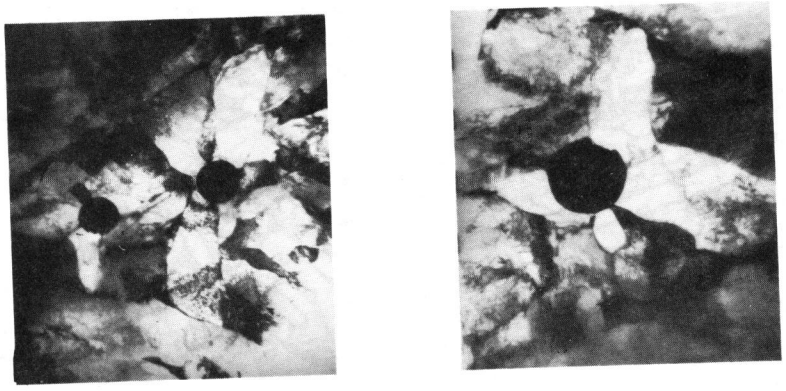

(a) (b)

Fig. 12 : Fine ferrite grains apparently nucleated at oxide inclusions – 48×10^{-3} % O_2 :
a) 7250 x, b) 14000 ×